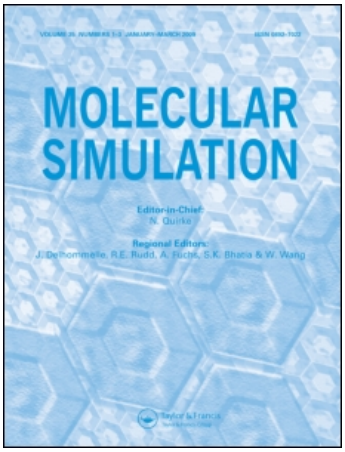

Molecular Simulation
Publication details, including instructions for authors and subscription information:
http://www.informaworld.com/smpp/title~content=t713644482

A Molecular Dynamics Simulation of an Aqueous Beryllium Chloride Solution

M. M. Probst[ab]; E. Spohr[ac]; K. Heinzinger[a]; P. Bopp[d]
[a] Max-Planck-Institut für Chemie (Otto-Hahn-Institut), Mainz, Germany [b] Institut für Anorganische und Analytische Chemie, Universität Innsbruck, Innsbruck, Austria [c] Department of Chemistry, University of California at Irvine, CA, USA [d] Institut für Physikalische Chemie, Rheinisch-Westfälische Technische Hochschule, Aachen, Germany

To cite this Article Probst, M. M. , Spohr, E. , Heinzinger, K. and Bopp, P.(1991) 'A Molecular Dynamics Simulation of an Aqueous Beryllium Chloride Solution', Molecular Simulation, 7: 1, 43 — 57
To link to this Article: DOI: 10.1080/08927029108022447
URL: http://dx.doi.org/10.1080/08927029108022447

Molecular Simulation, 1991, Vol. 7, pp. 43–57
Reprints available directly from the publisher
Photocopying permitted by license only

A MOLECULAR DYNAMICS SIMULATION OF AN AQUEOUS BERYLLIUM CHLORIDE SOLUTION

M.M. PROBST*, E. SPOHR†, K. HEINZINGER

Max-Planck-Institut für Chemie (Otto-Hahn-Institut), D-W-6500 Mainz, Germany

P. BOPP

Institut für Physikalische Chemie, Rheinisch-Westfälische Technische Hochschule, D-W-5100 Aachen, Germany

(*Received April 1990, accepted October 1990*)

A Molecular Dynamics simulation of a 1.1 molal aqueous $BeCl_2$ solution was performed with the flexible BJH model for water and a newly developed three-body potential for Be^{2+}–H_2O interactions derived from ab-initio calculations. The properties of the potential are discussed and radial distribution functions, angular distributions and dynamic properties of the solution like vibrational modes and hindered rotations are analyzed.

KEY WORDS: Molecular Dynamics simulation, aqueous $BeCl_2$ solution, three-body interactions, hydration shell structures, intramolecular frequencies, hydrogen bonding.

1. INTRODUCTION

The hydration shell structures of the alkaline earth ions Be^{2+}, Mg^{2+}, Ca^{2+} and Sr^{2+} have been investigated by Molecular Dynamics (MD) simulations and reported in a series of papers in recent years [1–4]. Be^{2+}, as the first member of this group in the periodic table, deserves special attention because it is a very small ion with a high electric field near to it. The ionic radius of Be^{2+} is about 0.27 Å while that of Mg^{2+} is 0.72 Å. Therefore, the assumption of pairwise additivity of the ion-water interaction energies is much less justified for the Be^{2+}–water system than for the other alkaline earth ions [5]. As in the preceding simulation of the $BeCl_2$ solution [1] pair potentials were employed, it seemed to be advisable to repeat this investigation by including three-body terms for the Be^{2+}–H_2O interaction.

Some characteristics of the potential energy surface and details of the simulation are given in sections 2 and 3. The results found for various structural and spectroscopic properties of the solution are discussed in section 4 in comparison with those of previous simulations of alkaline earth chloride solutions.

*Permanent address: Institut für Anorganische und Analytische Chemie, Universität Innsbruck, A-6020 Innsbruck, Austria.
†Present address: Department of Chemistry, University of California at Irvine, CA 92717, USA.

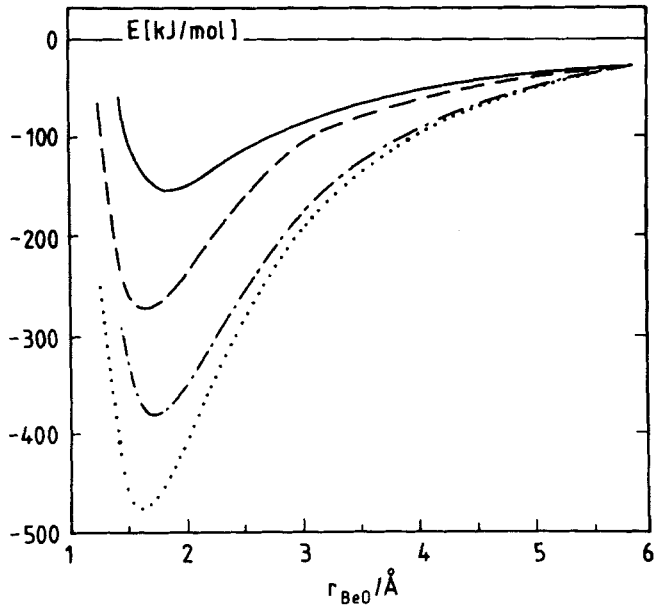

Figure 1 SCF (full; dashed) and 2-body potential energies (dash-dotted; dotted) for $Be^{2+}(H_2O)_3$–H_2O (dashed; dotted) and $Be^{2+}(H_2O)_5$–H_2O (full; dash-dotted) as a function of the Be–O distance.

2. THE ENERGY SURFACE IN THE Be^{2+}–H_2O SYSTEM

Ab initio calculations of the Be^{2+}–H_2O potential surface [1] yield a value of -570 kJ/mol in the global minimum. Due to well known effects like charge transfer from water to the ion and polarization of the water molecules the total binding energy in a $Be^{2+}(H_2O)_n$ cluster is less than n times the Be^{2+}–H_2O interaction at the given Be–O distance plus the water–water interaction. Rather similar total binding energies of 1670 kJ/mol and 1737 kJ/mol result for the geometry optimized $Be^{2+}(H_2O)_4$ and $Be^{2+}(H_2O)_6$ clusters, respectively, whereas the assumption of additivity strongly favours $Be^{2+}(H_2O)_6$ (2053 kJ/mol vs. 2568 kJ/mol).

In order to show the difference between the sum of the pair potentials and the many-body potential we have calculated the binding energy of one H_2O molecule in tetrahedral and octahedral Be^{2+} clusters as a function of its Be–O distance for an orientation where the dipole moment vector points away from the cation. The remaining 3, respectively 5, water molecules were kept 'frozen' at the optimized geometry of the cluster. Figure 1 shows the corresponding potential energy curves obtained by means of the two-body approximation and with full Hartree-Fock calculations. While the Hartree-Fock interaction energy between one water molecule and the remaining $Be^{2+}(H_2O)_5$ complex is less than 160 kJ/mol, the attraction between the two subsystems is more than doubly overestimated in the pair approximation. A similar difference is found for the tetrahedral complex.

Although simulation studies incorporating many-body effects mainly by using dipolar polarizable models are becoming feasible [6] it seems—for reasons of consistency—better to improve the reliability of the results of the $BeCl_2$ simulation by taking

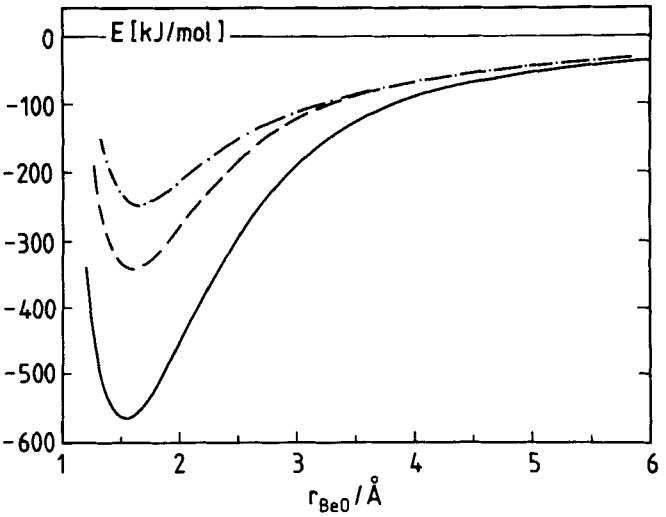

Figure 2 Effective Be^{2+}–H_2O energy curves for tetrahedral (dashed) and octahedral (dash-dotted) clusters (Eq. (1)) and the two-body Be^{2+}–H_2O potential (full).

the nonadditive effects into account. In principle, this can be done by using an 'effective potential' that includes many-body effects in an averaged way or by incorporating them explicitly. We know of only two previous investigations that used ion-water potentials improved in such a way for simulations of aqueous solutions. The first approach was taken by Curtiss *et al.* [7] in Md simulations of aqueous Fe^{2+} and Fe^{3+} while the second one was employed in a recent MC simulation on hydrated Li^+ by Corongiu *et al.* [8].

In order to get some information on the effective interaction energy between the Be^{2+} alone and one water molecule in its hydration shell, we subtracted the water–water interactions from the Hartree-Fock energy curves of Figure 1:

$$E(Be^{2+} - H_2O)_{eff} = E(Be^{2+}(H_2O)_{n-1} - H_2O) - E(H_2O)_{n-1} - H_2O) \quad (1)$$

For the case $n = 1$, from which the normal pair potential results and for $n = 4$ and $n = 6$, the energy curves are shown in Figure 2. The effective energy curves for $Be^{2+}(H_2O)_4$ and $Be^{2+}(H_2O)_6$ are close compared to the two-body curve but their minima still differ by about 80 kJ/mol. Under the assumption that nonadditive effects in the water–water interaction play a minor role for the total energy, this indicates that going from $Be^{2+}(H_2O)_4$ to $Be^{2+}(H_2O)_6$ additional charge transfer and saturation effects occur. While an average of the potential curves for $n = 4$ and $n = 6$ probably would give an accuracy comparable to the two-body potentials for Ca^{2+} or Sr^{2+}, we decided to incorporate non-additive terms directly into our cation–water potential as effective potentials always trade off some accuracy against computational advantages.

3. DETAILS OF POTENTIAL AND SIMULATION

We used the ion–water and ion–ion two-body potentials from ref. [1] which were derived from *ab initio* calculations and augmented the beryllium-water potential with an additional three-body term as reported recently [9].

The *ab initio* calculations were performed using basis sets of double-zeta quality (DZP). Single points were checked using triple-zeta basis sets (TZP) [10]. The basis sets of all atoms contained one set of polarization functions. The TZP binding energies are up to 5% higher than the DZP ones. For the three-body energies (which are always positive) TZP gives values that are about 12% larger than the DZP ones. For example, a typical conformation of two water molecules with the water dipole vector pointing away from the Be^{2+}, an O(1)–Be^{2+}–O(2) angle of 109°, $r_{BeO(1)} = 1.6$ Å and $r_{BeO(2)} = 1.8$ Å gives a DZP binding energy of 989 kJ/mol with a three-body part of 92 kJ/mol whereas the TZP value is 1039 kJ/mol with a three-body part of 105 kJ/mol. In view of the relatively small differences between the more accurate TZP values and the DZP results, in order to be consistent with [1], we based the calculation of our analytical potential on the latter ones.

The basis set superposition error for the DZP case was checked for by the counterpoise method and found to be in the order of 3% of the bindng energy and in the same order for the three-body energy. Nearly no basis set superposition error was found for the triple-zeta basis set.

The three-body part of the energy, E_{3b}, was extracted from the total energy of about 150 H_2O–Be^{2+}–H_2O triplets according to:

$$E_{3b} = E[Be^{2+}(H_2O)_2] - E[Be^{2+} - H_2O(1)] - E[Be^{2+} - H_2O(2)] - E[(H_2O)_2] + E[Be^{2+}] + 2E[H_2O], \quad (2)$$

where all energies on the right-hand side are total energies. This three-body energy has been fitted to the following analytical expression:

$$E_{3b} = A[B + (\pi - \alpha)^2]^2 \exp[-C(r_1^2 + r_2^2)], \quad (3)$$

where α denotes the O(1)–Be^{2+}–O(2) angle and r_1 and r_2 the distances between Be^{2+} and the oxygen atoms of the two water molecules. The functional form reflects the facts that the three-body energy decays fast with increasing distance of each oxygen from the Be^{2+} and that it is strongly dependent on the O–Be–O angle. Since the energy surface was found to be rather smooth, 150 H_2O–Be^{2+}–H_2O triplets were sufficient to scan the two O–Be distances and the O–Be–O angles. In all configurations, the angle θ between the water dipole moment vector and the vector pointing from the oxygen atom towards the ion (see insertion in Figure 5) was 180%. This, of course, limits the accuracy of the potential function for other configurations but we do not consider this a disadvantage since the two-body part of the potential shows that large deviations of θ from 180° are energetically very unfavourable.

Least square fitting to Eq. (3) and a modification of the Parameter C to approximately incorporate higher-order terms gave $A = 11.16$ kJ/mol, $B = -0.192$, and $C = 0.25$ Å^{-2} for the three free parameters [9]. The dependence of E_{3b} on distance and orientation is visualized in Figure 3. For linear O–Be–O arrangements, E_{3b} is almost constant within $1.5 > r_{BeO} > 1.8$. It, however, increases strongly if the O–Be–O angle gets smaller and then becomes more distance dependent, too.

In spite of the fact that the inclusion of the three-body term is only a first step towards very accurate potentials and although the many-body expansion of the energy is certainly not converged completely after the three-body term, this one is by far the most important correction of the pair potential. The higher order contributions seem to be of similar size as the uncertainties in the other potentials employed in the simulation.

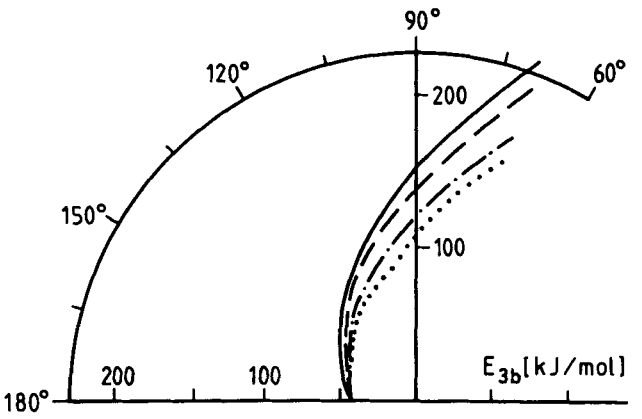

Figure 3 Polar plot of the dependency of E_{3b} on the O–Be–O angle for four different values of $r_{BeO(1)} = r_{BeO(2)}$: 1.5 Å (full); 1.6 Å (dashed); 1.7 Å (dash-dotted); 1.8 Å (dotted).

A technical detail deserves to be mentioned. In order to avoid inhomogenities of the forces at the cut-off radii normally the so-called "shifted force method" is used. This means that the original potential is modified by addition of a linear term and a constant so that both energy and force become zero at the radius of the cut-off sphere. This simple method is not directly extensible to many-body potentials and as a substitute we multiplied our three-body potential with a term T given by:

$$T = \{1 - \exp[D(r_c - r_1)^n]\} \cdot \{1 - \exp[D(r_c - r_2)^n]\} \quad (4)$$

It can be seen that the damping factor T ensures that the potential and its derivative are exactly zero if $r_1 = r_c$ or $r_2 = r_c$. Values of $D = 0.5$ and $n = 4$ ensure that T is different from one only if the cut-off radius is approached.

The basic cube contained 200 flexible BJH water molecules [11], 4 Be^{2+} and 8 Cl^-. The equilibration period of our simulation was started with a configuration from reference [1]. The long range Coulombic interactions were treated by the Ewald method while for the non-Coulombic interactions the shifted force method was employed with a cutoff distance of 9.2 Å, half of the sidelength of the basic periodic cube. After about 5000 time steps of equilibration, the final collection of data was performed for 12500 time steps of 0.25 fs each. The average temperature was 290 K. No rescaling of velocities was performed in order to obtain large time windows for the autocorrelations functions. The total energy was stable to better than 0.2% from the beginning to the end of the simulation.

4. RESULTS OF THE SIMULATION AND DISCUSSION

4.1 Radial Distribution Functions

The radial distribution functions (RDF's) for Be–O and Be–H have already been depicted in reference [9]. The figure is not repeated here but the characteristic values for $g_{BeO}(r)$ and $g_{BeH}(r)$ are given in Table I (see also Figure 4). Different from the simulation with the two-body potential [1] the hydration number of Be^{2+} is now found to be four and, accordingly, the number of nearest neighbor hydrogen atoms is eight.

Table 1 Characteristic values of the cation-water radial distribution functions, where R_i, r_{Mi} and r_{mi} are the distances where for the i^{th} time $g_{\alpha\beta}(r)$ is unity, has a maximum, or minimum, respectively.

α	β	R_1	r_{M1}	$g_{\alpha\beta}(r_{M1})$	R_2	r_{m1}	$g_{\alpha\beta}(r_{m1})$	$n_{\alpha\beta}(r_{m1})$	r_{M2}	$g_{\alpha\beta}(r_{M2})$
Be	O	1.62	1.75	23.2	1.90	2.02	0.0	4.0	4.27	3.2
Be	H	2.36	2.52	7.1	2.70	2.90	0.0	8.0	4.55	2.2

Except for a slight decrease in the height and a narrowing of the first peak in $g_{BeO}(r)$ connected with the smaller hydration number, all the other characteristic values given in Table I are not significantly different from the previous simulation. The same is true for the chloride-water and water–water RDF's. Therefore, they are not repeated here. They can be found in reference [1]

Since the only significant difference between the results of the simulations with and without the three-body potential is the change in the coordination number of Be^{2+} from six for four, it seems to be of interest, to investigate the sensitivity of the Be^{2+} coordination number on the potential. For this purpose, several molecular dynamics

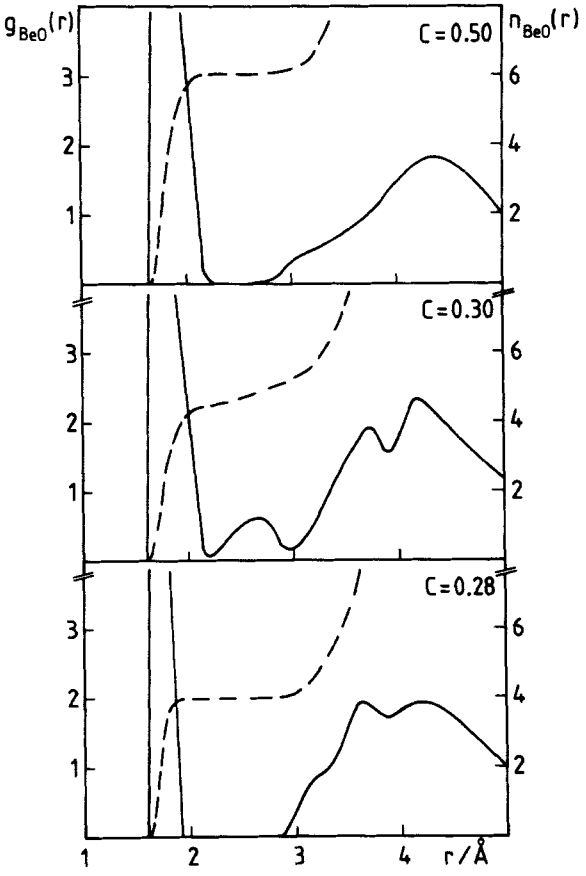

Figure 4 Beryllium-oxygen radial distribution functions (full) and running integration numbers (dashed) from simulations with three-body potentials for three different parameters C in Equation (3).

simulations of a few thousand timesteps each were performed. They showed no change in the hydration number when C (Equation (3)) was varied from 0.19 to 0.30. Only if values of about 0.30 and larger were used, the three-body potential became so weak that the coordination number changed again in to six within a few hundred timesteps. This is demonstrated in Figure 4 where the RDF's and the corresponding running integration numbers, $n(r)$, for simulation runs with $C = 0.5$, $C = 0.3$ and $C = 0.28$ are depicted. While the first and the last one indicate clearly coordination numbers of six and four, respectively, the simulation for the limiting case $C = 0.3$ shows water molecules moving between first and second hydration shell. Since the accuracy of our *ab initio* data leads to C values well below 0.3, it can be concluded that all theoretical and experimental [1] evidence now points towards a coordination number of four for Be^{2+} under the conditions studied.

4.2 Orientation of the Water Molecules

The distributions of cos θ for the water molecules in the first hydration shells of Be^{2+} and Cl^- are shown in Figure 5. θ is defined as the angle between the dipole moment direction of the water molecule and the vector pointing from the oxygen atom toward the center of the ion. Figure 5 shows for Be^{2+} a strong preference for a trigonal orientation. The distribution is significantly narrower than that for the other alkaline earth ions and for Be^{2+} with the two body potential [1]. The water molecules in the first hydration shell of Cl^- form preferentially linear hydrogen bonds, with a distribution which is very similar to the one found for the other alkaline earth chloride solutions [1].

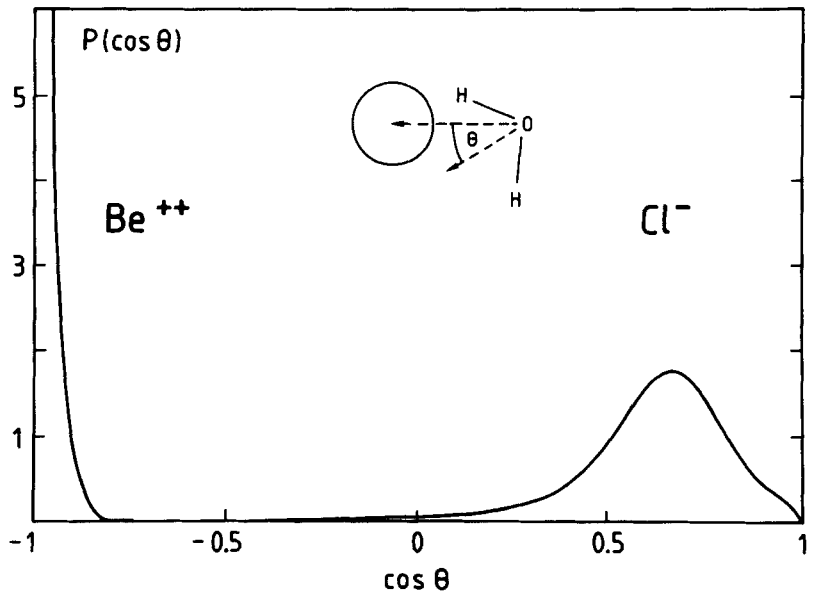

Figure 5 Distribution of cos θ for the water molecules in the hydration shells of the ions. θ is defined in the insertion.

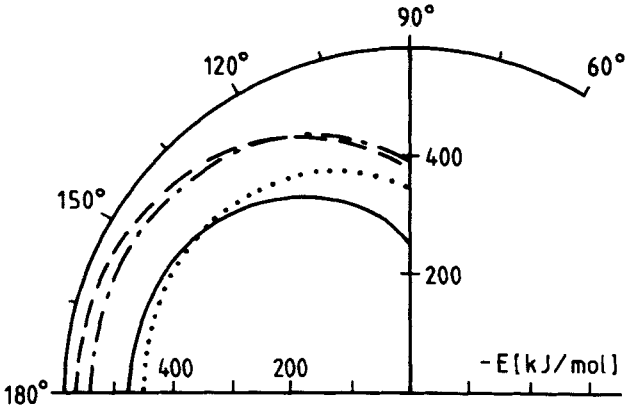

Figure 6 Polar plot of the Be^{2+}–H_2O interaction energy as a function of θ, where θ is defined in the insertion of Figure 5, for four different ion-oxygen distances. The denotations are the same as in Figure 3.

It is of interest to investigate if this strong preference for $\theta = 180°$ results from the potential or if the interaction with the other water molecules is responsible for it. For this purpose the angular dependency of the potential of the Be^{2+}–H_2O interaction energy is plotted in Figure 6 as a function of θ for four different Be–O distances. The restriction of the cos θ distribution to values smaller than -0.8 for Be^{2+} (Figure 5) is in accordance with this potential but the very strong preference for $\theta = 180°$ results from the interactions between the water molecules in the first and second hydration shell.

4.3 Hydration Shell Structure of Be^{2+}

From the knowledge of the positions of all particles as a function of time, provided by the MD simulation, the geometrical arrangement of the water molecules in the first hydration shell of Be^{2+} has been deduced by calculating the distribution of cos ϑ where ϑ is defined as the O–Be–O angle. The result is shown in Figure 7, where only the oxygen atoms of the water molecules in the first hydration shell of Be^{2+} are included in the distribution. It is centered at the tetrahedral angle of 109.5° as expected for a hydration number of four. The halfwidth of the distribution corresponds to about 20°. It shows that even for an ion as small as Be^{2+} the hydration shell is rather flexible.

4.4 Self-Diffusion Coefficients

The self-diffusion coefficients for the various subsystems in the solution have been calculated according to the Green–Kubo relation from the integral over the velocity autocorrelation functions in the limit $t \to \infty$. The values for Be^{2+} and Cl^- are found to be (0.7 ± 0.2) and $(1.2 \pm 0.2) \cdot 10^{-5} cm^2 s^{-1}$, respectively. The errors are estimated from the noise in the velocity autocorrelation functions after their decay to zero. This result for the chloride ion is in the limits of statistical uncertainty the same as the one calculated from the simulations of a 1.1 molal $SrCl_2$ and several 2.2 molal alkali chloride solutions [4] and indicates that at moderate concentrations D_{Cl^-} does not

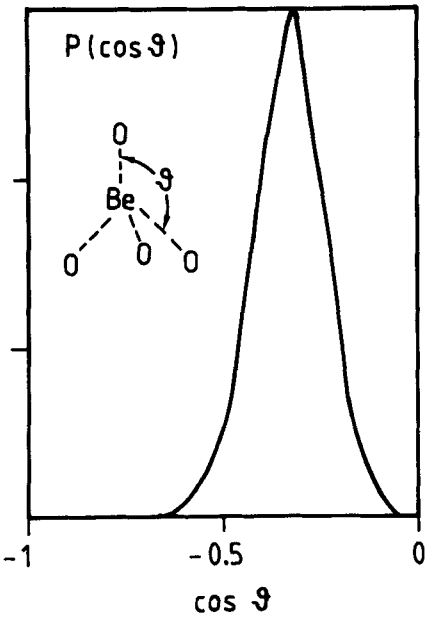

Figure 7 Distribution of cos ϑ for the water molecules in the first hydration shell of Be^{2+}. ϑ is defined in the insertion.

depend strongly on the cation. The self-diffusion coefficient for Be^{2+} is in the limits of error the same as calculated for Sr^{2+} in the 1.1 molal $SrCl_2$ solution [4] and for Li^+ in the 2.2 molal LiI solution [12]. It is only about half of that found for Cl^-. The strong interactions between the small and/or doubly charged cations and the surrounding water molecules lead to a large effective mass of the cations which results in significantly smaller self-diffusion coefficients than those of the weakly hydrated anions Cl^- and I^- [13].

The simulation permits the calculation of the self-diffusion coefficients separately for the three water subsystems in the $BeCl_2$ solution. The values for the hydration water of Be^{2+}, of Cl^-, and bulk water are found to be (0.8 ± 0.2), (1.2 ± 0.2), and $(1.3 \pm 0.2) \cdot 10^{-5} cm^2 s^{-1}$, respectively. A water molecule is considered to belong to the first hydration shell of an ion if it ion–O distance is smaller than r_{m1} (Table 1). the subdivision into the three classes is carried out at each correlation origin. The exchange of water molecules between the three classes is negligible during the typical lengths of the correlations. There is no difference in the limits of statistical uncertainty between bulk water and the hydration water of Cl^- presumably because of the relatively weak interaction between the chloride ion and its hydration shell. On the contrary, the very strong interactions between Be^{2+} and its hydration shell water molecules lead in the limits of error to the same self-diffusion coefficient for both. This result is different from that for Li^+ and Sr^{2+}. The smaller charge or the larger size of these ions compared with Be^{2+} mean weaker interactions. Therefore, the self-diffusion coefficients of the water molecules in the first hydration shells of Li^+ and Sr^{2+} are larger than those of the ions by a factor of about 2.5 and 1.5, respectively [4,12].

4.5 Librational and Vibrational Motions of the Water Molecules

In order to separate the various librational and vibrational modes of the water molecules the following scheme has been employed [14]: The instantaneous velocities of the two hydrogen atoms in the center-of-mass system are projected onto the instantaneous unit vectors: i) in direction of the corresponding O–H bond ($\mathbf{u}_1$ and $\mathbf{u}_2$), ii) perpendicular to the O–H bonds in the plane of the molecule ($\mathbf{v}_1$ and $\mathbf{v}_2$), and iii) perpendicular to the plane of the molecule ($\mathbf{p}_1$ and $\mathbf{p}_2$).

Using capital letters to denote the projections of the hydrogen velocities onto the corresponding unit vectors, the following quantities are defined:

$$\begin{aligned} Q_1 &= U_1 + U_2 \quad R_x = V_1 - V_2 \\ Q_2 &= V_1 + V_2 \quad R_y = P_1 + P_2 \\ Q_3 &= U_1 - U_2 \quad R_z = P_1 - P_2 \end{aligned}$$

where Q_1, Q_2, and Q_3 describe approximately the three normal mode vibrations usually referred to as symmetric stretch, bend, and asymmetric stretch, respectively. R_x, R_y, and R_z approximate the instantaneous rotations around the three principal axes of the water molecule, as defined in the insertion of Figure 8. The Fourier transformations of the normalized autocorrelation functions of these quantities result in the spectral densities of the corresponding modes. They have been calculated separately for the three water subsystems and are shown for the librational and vibrational motions in Figures 8 and 9, respectively. While this procedure is an approximate one, it has been shown to describe with a sufficient accuracy the changes in the vibrational frequencies of the anharmonic oscillators perturbed by the fluctuating environment of a molecule [4,14,15].

In Table 2 the intramolecular geometries of the water molecules in the hydration shell of Be^{2+} as well as the positions of the maxima in the spectral densities of the librations and intramolecular vibrations are presented as calculated from the simulations with the two- and three-body potentials. They are compared with the results for pure water which are in the limits of statistical uncertainty the same as for the bulk water in the 1.1. molal $BeCl_2$ solution.

It can be seen from Figure 8 that the spectral densities of the librations around the x- and z-axes are quite similar for bulk water and the hydration water of the anion while for the y-axis the anion causes a slight blueshift, similar to that found in the

Table 2 Intramolecular geometries and the frequencies of the peak maxima in the librational and vibrational spectral densities for pure water and for the water molecules in the first hydration shell of Be^{2+} from simulation of a 1.1 molal $BeCl_2$ solution with a two and a three-body potential for the Be^{2+}-water interactions. The uncertainties in the positions of the maxima are estimated to be $\pm 15\,cm^{-1}$

	pure water	*hydration shell water of Be^{2+}*	
		two-body	*three-body*
r_{OH}[Å]	0.9760	0.9940	1.0059
∠ HOH[°]	100.3	96.9	93.9
R_x[cm^{-1}]	438	580	631
R_y[cm^{-1}]	590	765	807
R_z[cm^{-1}]	418	436	398
Q_1[cm^{-1}]	3475	3119	2907
Q_3[cm^{-1}]	3580	3176	3020

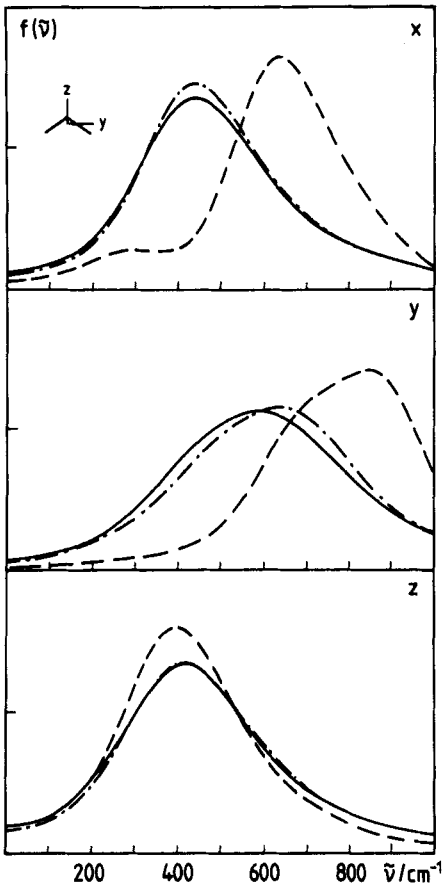

Figure 8 Spectral densities of the librations of the water molecules around its three main axes, calculated separately for the three water subsystems in the $BeCl_2$ solution: Bulk water (full), hydration water of the cation (dashed) and of the anion (dash-dotted) and given in arbitrary units.

$SrCl_2$ solution [4], which results from the slightly stronger hydrogen bond formed between Cl^- and water than between water and water which is also evident from the corresponding small redshift in the O–H stretching vibration shown in Figure 9. The strong Be^{2+}–water interaction causes a strong blueshift relative to bulk water of the librational motions of its hydration shell water molecules around the x- and y-axes. But the spectral densitiy around the dipole moment axis remains—not unexpectedly because of the orientation of the water molecules (Figure 5)—unchanged in the limits of statistical uncertainty.

It can be seen from Table 2 that the use of the three-body potential for the Be^{2+}–water interactions causes a blueshift of the librational frequencies around the x- and y-axes. This blueshift continues the trend from pure water along the alkaline earth ions with decreasing ion size [4,15]. But this further increase is surprising because the Be^{2+}–water interactions are weaker for the three-body than for the two-body potential, different from the trend with decreasing ion size. A possible explanation could be that the hydrogen bonds between the water molecules in the first

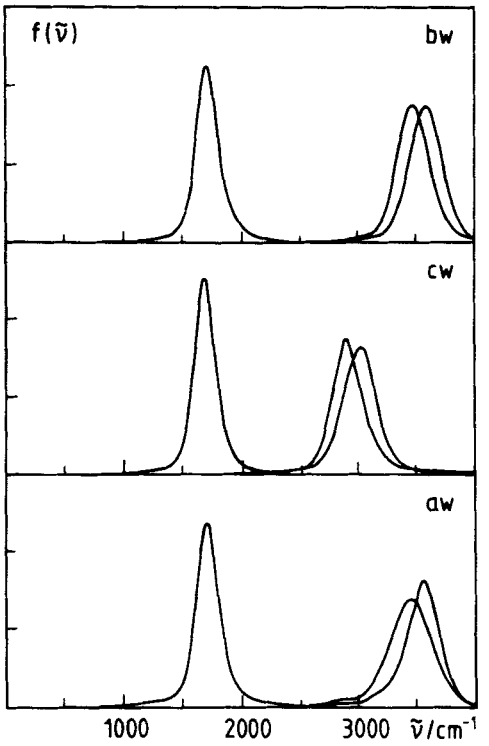

Figure 9 Spectral densities of the three intramolecular vibrations calculated separately for bulk water, hydration water of the cation and of the anion and given in arbitrary units. From low to high fequency: Q_2, Q_1 and Q_3.

and second hydration shell of Be^{2+} become stronger as a consequence of the change of the hydration number from 6 to 4 for the three-body potential and, in this way, overcompensate the weaker Be^{2+}-water interactions (see below). This change in the hydration number might also be responsible for the redshift of R_z because it means less steric hindrance for the rotational motions around the dipole moment axis in the case of the trigonal orientation. The reduced hindrance seems to overcompensate the stronger hydrogen bond effect. This explanation is in accordance with the results for the other alkaline earth ions. In the case of Sr^{2+} and Ca^{2+}, R_z has been found smaller than 400 cm^{-1} while it is for Mg^{2+} the same as for pure water [4,15].

The three intramolecular vibrations of the water molecules are presented in Figure 9 separately for bulk water, hydration water of Be^{2+} and Cl^-. The bending frequency is the same in the limits of statistical uncertainty for all three subsystems and is, therefore, omitted in Table 2. The symmetric and the asymmetric stretching vibrations are well separated. Their small redshift for the hydration water of Cl^- relative to bulk water is similar to what has been calculated from simulations of other akaline earth chloride solutions [4,15]. A strong readshift of about 560 cm^{-1} relative to pure water is found for both stretching modes in the hydration water of Be^{2+}. On the basis of the well-known empirical relationship between the intramolecular O–H distance and the frequencies of the O–H stretching modes of about 20000 cm^{-1}/Å [16] this redshift is in accordance with the increase of the O–H distance of about 0.03 Å (Table 2).

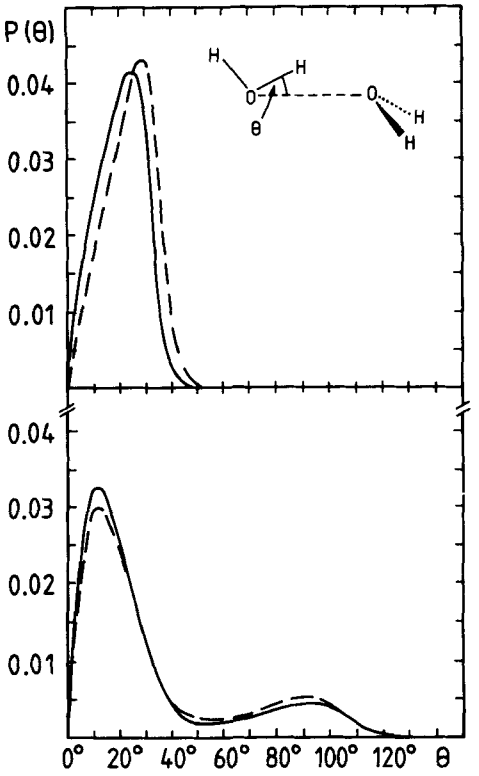

Figure 10 Normalized distributions of the hydrogen bond angle θ – which is defined in the insertion – as calculated from simulations with the three-body (full) and two-body (dashed) potential for the Be^{2+}–water interactions. Upper curves: hydrogen bond angles between first and second hydration shell of Be^{2+} only. Lower curves: hydrogen bond angles between all bulk water molecules in the solution with O–O distances smaller than 3.35 Å.

The frequency shift of Q_1 and Q_3 as calculated from the simulation with the two-body potential (Table 2) follows the tendency of an increased redshift with the decrease in ion size found for the alkaline earth ion series [4,15]. Although in accordance with the empirical rule mentioned in the preceding paragraph a further increase of the redshift resulting for the three-body potential is rather unexpected because of the weaker Be^{2+}–water interaction in this case (Figure 2). Similar to R_x and R_y discussed above this result seems to indicate again a stronger hydrogen bond formation between first and second hydration shell of Be^{2+} for the three-body potential.

In order to check whether this conclusion is justified the hydrogen bond angle distribution, $P(\theta)$, where θ is defined in the insertion of Figure 10, between the water molecules in the first shell (Be^{2+}–O distances smaller than 2.4 Å) and the second shell (O–O distances smaller than 3.35 Å) has been calculated from the simulations with the two- and the three-body potential. The result is presented in the upper part of Figure 10. Undoubtedly, the distribution for the two-body potential is shifted to larger angles. To quantify those results the average number of hydrogen bonds has been calculated under the assumption that a hydrogen bond is formed if θ is smaller than

20°. This choice is quite arbitrary but leads to a reasonable upper limit for the energy of the hydrogen bonded dimer [17]. With this definition the average number of hydrogen bonds is calculated from Figure 10 to be 0.84 and 0.58 for the three- and two-body potentials, respectively. As only donative hydrogen bonds are counted each water molecule can form only two bonds. The percentages of water molecules in the first shell which form simultaneously zero, one or two hydrogen bonds are 31(49), 53(42) and 16(9), respectively, where the numbers in parentheses result from the simulations with the two-body potential.

It is obvious from Figure 10 and these numbers that the simulation with the three-body potential for the Be^{2+}–water interactions leads to significantly stronger hydrogen bonds between the water molecules in the first and second hydration shell of Be^{2+}. It has been demonstrated by Kleeberg *et al.* [18] that the influence of the cations on the O–H stretching vibration increases proportionally with the frequency shift due to the hydrogen bond and that the proportionality factor increases with the strength of the cation–water interactions. Therefore, it can be understood qualitatively that there is an increase in the frequency shift for the three-body potential although the minimum of the Be^{2+}–water potential is lower in the two-body case.

In the lower part of Figure 10 $P(\theta)$ is drawn for the case where all water molecules outside of the first hydration shell serve as reference particles (Be^{2+}–O distance larger than 2.4 Å), again with the restriction of O–O distances smaller than 3.35 Å. The resulting average numbers of hydrogen bonds for the three-body (full) and the two-body (dashed) potential are calculated to be 1.00 and 0.89, respectively. The percentage of water molecules which form simultaneously zero, one and two hydrogen bonds are 25(32), 49(47) and 26(21), respectively, where the numbers in parenthesis are again from the simulation with the two-body potential. Although the differences between the two curves for bulk water are smaller than those for the hydration water of Be^{2+}, they are still significant. A comparison with $P(\theta)$ for pure BJH water (Figure 10 in reference [1]) shows that the use of a three-body potential for the Be^{2+}–water interactions leads to a hydrogen bond angle distribution for bulk water which is in between that for pure water and that resulting from the two-body potential. Obviously the introduction of the three-body forces leads not only to a reduction of the hydration number but also to an energetically more favourable water structure which stabilizes the tetrahedral hydration sphere of the beryllium ion.

5. CONCLUSIONS

The MD simulation reported here shows that potentials including three-body terms can be used in practice advantageously in simulations of aqueous systems. Besides the dramatic change in the hydration number many other quantities show small but significant changes. Some vibrational and librational frequencies of the water molecules in the first hydration shell of Be^{2+} show larger shifts than those found for all other ions investigated so far.

Acknowledgement

Financial support by Deutsche Forschungsgemeinschaft and the Fonds der Chemischen Industrie (P.B.) is gratefully acknowledged.

References

[1] T. Yamaguchi, H. Ohtaki, E. Spohr, G. Pálinkás, K. Heinzinger and M.M. Probst, "Molecular Dynamics and x-ray diffraction study of aqueous beryllium(II) chloride solutions", *Z. Naturforsch.*, **41a,** 1175 (1986).

[2] W. Dietz, W.O. Riede and K. Heinzinger, "Molecular Dynamics simulation of an aqueous $MgCl_2$ solution. Structural results", *Z. Naturforsch.*, **37a,** 1038 (1982).

[3] M.M. Probst, T. Radnai, K. Heinzinger, P. Bopp and B.M. Rode, "Molecular Dynamics and x-ray investigation of an aqueous $CaCl_2$ solution", *J. Phys. Chem.*, **89,** 753 (1985).

[4] E. Spohr, G. Pálinkás, K. Heinzinger, P. Bopp and M.M. Probst," A Molecular Dynamics study of an aqueous $SrCl_2$ solution", *J. Phys. Chem.*, **92,** 6754 (1988).

[5] M.M. Probst, J. Limtrakul and B.M. Rode, "A study of the Be^{2+}-H_2O system by means of *ab initio* calculations", *Chem. Phys. Lett.*, **132,** 370 (1986).

[6] J.A.C. Rullmann and P.Th. van Duijnen, "A polarizable water model for calculation of hydration energies", *Mol. Phys.*, **63,** 451 (1988).

[7] L.A. Curtiss, J.W. Halley, J. Hautman and A. Rahman, "Nonadditivity of *ab initio* pair potentials for molecular dynamics of multivalent transition metal ions in water", *J. Chem. Phys.*, **86,** 2319 (1987).

[8] G. Corongiu, M. Migliore and E. Clementi, "Hydration free energy for Li^+ at infinite dilution with a three-body *ab initio* potential", *J. Chem. Phys.*, **90,** 4629 (1989).

[9] M.M. Probst, E. Spohr and K. Heinzinger, "On the hydration of the beryllium ion", *Chem. Phys. Lett.*, **161,** 405 (1989).

[10] T.H. Dunning, "Gaussian basis functions for use in molecular calculations. I. Contraction (9*s*5*p*) atomic basis sets for the first row atoms", *J. Chem. Phys.*, **53,** 2823 (1970).

[11] P. Bopp, G. Jancsó and K. Heinzinger, "An improved potential for non-rigid water molecules in the liquid phase", *Chem. Phys. Lett.*, **98,** 129 (1983).

[12] Gy.I. Szász, K. Heinzinger and W.O. Riede, "Self-diffusion and reorientational motion in an aqueous LiI solution. A Molecular Dynamics study", *Ber. Bunsenges, Phys. Chem.*, **85,** 1056 (1981).

[13] Gy.I. Szász and K. Heinzinger, "A Molecular Dynamics study of the translational and rotational motions in an aqueous LiI solution", *J. Chem. Phys.*, **79,** 3467 (1983).

[14] P. Bopp, "A study of the vibrational motions of water in an aqueous $CaCl_2$ solution", *Chem. Phys.*, **106,** 205 (1986).

[15] P. Bopp, "Molecular Dynamics computer simulations of solvation in hydrogen bonded systems", *Pure Appl. Chem.*, **59,** 1071 (1987).

[16] S.I. LaPlaca, W.C. Hamilton and A.J. Prakash, "On a nearly proton-ordered structure for ice IX", *J. Chem. Phys.*, **58,** 567 (1973).

[17] K. Heinzinger and G. Pálinkás, "Interactions of water in ionic hydrates", in *Interaction of Water in Ionic and Nonionic Hydrates*, H. Kleeberg, ed., Springer Verlag, Berlin-Heidelberg-New York, 1987, p. 1.

[18] H. Kleeberg, G. Heinje and W.A.P. Luck, "Influence of alkali cations on the infrared spectra of water molecules in aprotic solvents", *J. Phys. Chem.*, **90,** 4427 (1986).